HHS Public Access

Author manuscript

Cell. Author manuscript; available in PMC 2017 August 02.

Modeling Rett Syndrome Using TALEN-Edited *MECP2* Mutant Cynomolgus Monkeys

Yongchang Chen[1,3,12,13,14,*], **Juehua Yu**[2,13], **Yuyu Niu**[1,3,12,13], **Dongdong Qin**[5,13], **Hailiang Liu**[2,13], **Gang Li**[6], **Yingzhou Hu**[5], **Jiaojian Wang**[7], **Yi Lu**[8], **Yu Kang**[1,3,12], **Yong Jiang**[9], **Kunhua Wu**[9], **Siguang Li**[2], **Jingkuan Wei**[1,3], **Jing He**[1,3], **Junbang Wang**[2], **Xiaojing Liu**[2], **Yuping Luo**[2], **Chenyang Si**[1,3,12], **Raoxian Bai**[1,3], **Kunshan Zhang**[2], **Jie Liu**[2], **Shaoyong Huang**[1,3], **Zhenzhen Chen**[1,3], **Shuang Wang**[1,3], **Xiaoying Chen**[2], **Xinhua Bao**[10], **Qingping Zhang**[10], **Fuxing Li**[2], **Rui Geng**[2], **Aibin Liang**[2], **Dinggang Shen**[6], **Tianzi Jiang**[7,11], **Xintian Hu**[5], **Yuanye Ma**[1,3], **Weizhi Ji**[1,3,12,*], and **Yi Eve Sun**[2,4,*]

[1]Yunnan Key Laboratory of Primate Biomedicine Research, Institute of Primate Translational Medicine, Kunming University of Science and Technology, Kunming 650500, China

[2]Translational Stem Cell Research Center, Tongji Hospital, Tongji University School of Medicine, Shanghai 200065, China

[3]Yunnan Provincial Academy of Science and Technology, Kunming 650051, China

[4]Department of Psychiatry and Biobehavioral Sciences, UCLA Medical School, Los Angeles, CA 90095, USA

[5]Key Laboratory of Animal Models and Human Disease Mechanisms of the Chinese Academy of Sciences & Yunnan Province, Kunming Institute of Zoology, Chinese Academy of Sciences, Kunming 650223, China

[6]Department of Radiology and BRIC, University of North Carolina at Chapel Hill, Chapel Hill, NC 27599, USA

[7]Key Laboratory for NeuroInformation of the Ministry of Education, School of Life Science and Technology, University of Electronic Science and Technology of China, Chengdu 625014, China

[8]Department of Medical Imaging, the First Affiliated Hospital, Kunming Medical University, Kunming 650032, China

[9]The First People's Hospital of Yunnan Province and The Affiliated Hospital of Kunming University of Science and Technology, Kunming 650032, China

[13]These authors contributed equally

[14]Lead Contact

[10]Department of Pediatrics, Peking University First Hospital, Beijing 100034, China

[11]National Laboratory of Pattern Recognition, Brainnetome Center, Institute of Automation, Chinese Academy of Sciences, Beijing 100190, China

[12]Kunming Enovate Institute of Bioscience, Kunming 650000, China

Summary

Gene-editing technologies have made it feasible to create nonhuman primate models for human genetic disorders. Here, we report detailed genotypes and phenotypes of TALEN-edited *MECP2* mutant cynomolgus monkeys serving as a model for a neurodevelopmental disorder, Rett syndrome (RTT), which is caused by loss-of-function mutations in the human *MECP2* gene. Male mutant monkeys were embryonic lethal, reiterating that RTT is a disease of females. Through a battery of behavioral analyses, including primate-unique eye-tracking tests, in combination with brain imaging via MRI, we found a series of physiological, behavioral, and structural abnormalities resembling clinical manifestations of RTT. Moreover, blood transcriptome profiling revealed that mutant monkeys resembled RTT patients in immune gene dysregulation. Taken together, the stark similarity in phenotype and/or endophenotype between monkeys and patients suggested that gene-edited RTT founder monkeys would be of value for disease mechanistic studies as well as development of potential therapeutic interventions for RTT.

Graphical abstract
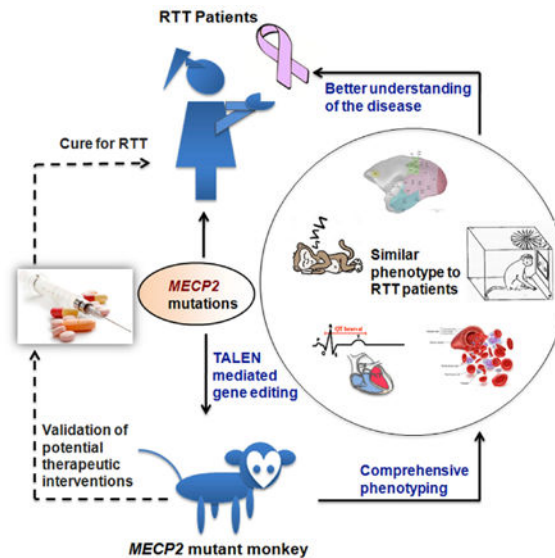
TALEN-edited MeCP2 mutant monkeys share phenotypes with Rett syndrome patients, providing a valuable model for studying disease mechanisms and for the development of potential therapeutics.

Introduction

Rett syndrome (RTT) is a progressive neurodevelopmental disorder that mostly manifests in girls with a morbidity rate of 1:10,000–1:15,000 (Amir et al., 1999). Almost 95% of RTT is believed to be caused by mutations of an X-linked gene methyl-CpG-binding protein 2 (*MECP2*) (Rett, 1966; Amir et al., 1999; Schanen et al., 1998). *MECP2* mutations are most often embryonic lethal for boys, except for very few, who are born with severe encephalopathy leading to death before 2 years of age (Schanen et al., 1998). RTT girls seem to have normal development for up to 6–18 months but manifest a series of symptoms associated with intellectual disability, loss of acquired language, and compromised cognitive, social, and motor skills, etc. (Hagberg et al., 1983).

As RTT is a monogenic disorder, genetic modification technologies have made it possible to develop animal models for further study. RTT animal models were first generated in mice and recently in rats (Chen et al., 2001; Guy et al., 2001; Stearns et al., 2007; Ricceri et al., 2008; Yang et al., 2013; Veeraragavan et al., 2016). It is interesting that RTT-related neurological phenotypes mostly occur in adult male rodents, which is different from the human disease (Lombardi et al., 2015; Patterson et al., 2016; Chen et al., 2001; Glaze, 2004; Guy et al., 2001). It is therefore conceivable that gene-edited nonhuman primates (NHPs) would serve as a better choice for modeling genetic neurological disorders including RTT (Jennings et al., 2016). Although monkeys and humans are different in many ways given that evolution has separated the Old World primate lineage into different paths, NHPs, such as rhesus and cynomolgus monkeys, still share high levels of genetic, physiological, social behavioral, and CNS developmental similarities with humans, making them suitable for the study of neurodevelopmental disorders (Shultz et al., 2011; Izpisua Belmonte et al., 2015)

In a previous study, we reported the successful application of TALEN-mediated mutagenesis to produce *MECP2* mutant monkeys (Liu et al., 2014), which opened up great opportunities for using monkey models to better understand RTT and to develop potential treatments for the disease. In this study, using the same technology, we generated additional *MECP2* mutants, from which we recapitulated embryonic lethality of mutant males and physiological and behavioral abnormalities of mutant females, including primate-unique eye tracking, which are seen with RTT patients. Moreover, brain imaging by MRI, MeCP2 protein measurements by semiquantitative western blotting, and transcriptome profiling of peripheral blood all demonstrated that these phenotypes (and/or endophenotypes) of the *MECP2* mutant monkeys were strikingly similar to RTT clinical manifestations, which can be used for disease mechanistic studies as well as development of potential therapeutic interventions for RTT.

Results

Generation of *MECP2* Mutant Monkeys via TALENs

In our previous report, one live female mutant monkey and three spontaneously aborted male mutant fetuses were generated using TALENs (Liu et al., 2014). After that, we generated another six live monkeys (four female mutants and two non-affected wild-type [WT] males) and five spontaneously aborted fetuses (two male mutants, two female mutants, one non-

affected WT female). The fact that all male mutant monkeys were embryonic lethal recapitulated the human disease (Chen et al., 2001; Guy et al., 2001) but different from *Mecp2* knockout mice. In this study, we gathered all available animals, i.e., five female mutants and five spontaneously aborted male fetuses from 41 surrogate recipients, and carried out the following studies (Figures 1A and 1B; Table S1).

Mutations of the *MECP2* gene from live monkeys and aborted fetuses were verified through T7EN1 cleavage, Sanger sequencing, and genome alignment. Live female mutants were further analyzed using Sanger sequencing of PCR-based clones from accessible tissues and compared with the reference for detection of missense, nonsense mutations, and/or indels on exon 3 of the *MECP2* gene (Table S2 and Figures 1C–1F). Distributions and frequencies of mutations for the #1 female *MECP2* mutation-carrying monkey (ID: 130958) can be found in the previous report (Liu et al., 2014). As for the other four newborn mutant females, mutations detected in placenta, blood, and skin were plotted in Figure 1C. All detected point mutations were plotted based on their positions and mutation rate in the entire targeted 351 bp of exon III.

MeCP2 protein levels in tissues (placentae and fibroblasts) of live monkeys and in brains (cortices) of aborted fetuses were overall lower in mutants as compared with those for WT controls (Figure 1G). Reduction of protein levels is shown in all five mutant monkeys (Figure 1G, a and b). Since it is not feasible to sample from cerebral cortices from live female monkeys due to technical and ethical concerns, we only compared MeCP2 levels in cortices from aborted fetuses from mutants and WT monkeys. Data from aborted male monkeys' cerebral cortices showed substantial reductions in MeCP2 levels (Figure 1G, c), which indirectly suggested that brain MeCP2 levels were also likely to be reduced in live mutant female monkeys. These data support the previous report that MeCP2 is a key regulator for neural development, which affects brain functions and behaviors (Chen et al., 2001).

Concerning potential off-target effects, we used a genome-wide TALEN off-target site prediction tool named TALENoffer (Grau et al., 2013; Liu et al., 2014). The statistical model of TALENoffer assumes that possible nucleotides on a target site can be traced from the repeat-variable di-residue of the corresponding repeat, which determines DNA binding specificity. Using a definite cutoff (TALENoffer score > -1.8) to define potential off-targets in the whole genome, a total of 41 exonic loci were predicted to be potential off-target sites (Table S3). The fragments of all the potential off-target loci from three pairs of TALENs were PCR amplified and subjected to Sanger sequencing. No mutations were found on these sites (Table S3). These data indicate that we did not detect off-target mutations on all 41 potential off-target sites from the four new monkeys and 11 WT control monkeys (Table S3).

MRI and EKG

Non-invasive neuroimaging is a very useful approach to assist diagnosis and monitoring longitudinal disease progression over time, which is particularly suitable for neural developmental disorders including RTT (Bjure et al., 1997; Naidu et al., 2001). We used MRI scanning to measure global or regional structural changes in brains of *MECP2* mutant monkeys. Similar MRI scanning has been done with RTT patients and reported (Bjure et al.,

1997; Naidu et al., 2001; Carter et al., 2008). In our study, MRI scanning was conducted three times with the first scanning performed at 7–8 months after birth, the second at 15 months, and the third at 20 months. A total of 60 subregions of each monkey's brain was segmented, and data were analyzed by both rank-sum test and false discovery rate (FDR) to correct for multiple comparisons. Mutant monkeys showed significantly reduced cortical gray matter (GM) volumes in 16 regions at least at one stage when compared to normal controls (Figure 2, a–j). Younger (8 months old) mutant monkeys had more cortical areas showing statistically significant reductions as compared to WT controls, whereas at the 20th month of age only bilateral occipital gyri, right inferior temporal gyrus, and right annectant gyrus displayed statistically significant reduction in volumes. In contrast, the difference in right annectant gyrus only became significant at the 20th month but not at younger ages (Figure 2, a–j). Widespread reductions in GM volumes of specific sub-cortical areas and region-specific white matter (WM) volumes were also apparent in *MECP2* mutant monkeys (Figure 2, k–p). Total brain GM and WM volumes, as well as total cortical volumes, total cortical surface areas, and average cortical thicknesses, were consistently smaller (with mean values) at all time points (i.e., 8, 15, and 20 months) in mutant monkeys, compared with WT controls, but the differences did not reach statistical significance (Figure S1). When these parameters were measured in a regional-specific manner, statistically significant alterations in mutant monkeys could be observed (Figures S1 and S2). Given that all five *MECP2* mutant monkeys have different repertoires of *MECP2* mutations, these results suggest that abnormal brain development in mutant monkeys, including reductions of subregional GM and WM volumes, specific cortical surface area, and cortical thickness, are likely due to MeCP2 deficiency. This is further supported by consistent abnormalities reported in previous MRI studies on human subjects with RTT (Naidu et al., 2001; Reiss et al., 1993; Carter et al., 2008; Subramaniam et al., 1997).

Abnormalities of electrocardiogram (EKG) records including QT interval (QTc) value and heart rate (HR) were found in patients (Neul et al., 2010). We tried EKG recording on five mutant monkeys and five WT controls. The data were analyzed by both Kolmogorov-Smirnov test and one-way ANOVA ($p > 0.05$). We found that mutant monkeys exhibited lower HR and longer QTc (Figure 3), which resembled RTT patients.

In addition, to investigate whether *MECP2* mutant monkeys have any differences in growth and development compared to age- and gender- matched WT controls, basic parameters including body weight, body length, head circumference, and biparietal diameter were measured every 3 months. There was no difference between mutants and WT monkeys in these parameters (Figure S3).

Behavioral Analyses

According to clinical diagnostic criteria for RTT (Hagberg et al., 2002; Neul et al., 2010; Katz et al., 2016), behavioral symptoms such as loss of acquired purposeful hand skills, loss of acquired spoken language, development of hand stereotype, inappropriate reactivity to environments, impaired locomotion, disruption in social interaction, social withdrawal, sleeping disorder, and reduced response to pain are often used to diagnose the disease before

genetic testing for *MECP2* mutations. Based on aforementioned symptoms, we used a battery of behavioral assays to analyze the phenotype of *MECP2* mutant monkeys.

Sleep pattern was classified into awake and asleep phases (including relaxed and transitional sleep). Frequency and duration will be an important index to evaluate the sleep pattern. Thus, we recorded and analyzed these two indexes in *MECP2* mutants and WT control monkeys. The total awake durations of mutants were found to be significantly longer while the total sleep durations were shorter than those of WT controls (Figure 4A, a). Remarkably, sleep in mutants was more fragmented than that in control monkeys, with more bouts of awaking and sleep (Figure 4A, b–d). It seemed difficult for mutant monkeys to have a continuous and longer-hour sleep, which is similar to RTT patients with abnormal circadian rhythms as well as *Mecp2* mutant mice (Li et al., 2015).

Pain Threshold Test—We examined monkeys' responses to heat stress and found that WT monkeys moved their feet frequently and constantly in response to rising temperatures, while mutants made no attempt to escape from the heating plate (Movie S1). When temperature rose further to certain threshold, both mutant monkeys and WT controls exhibited nocifensive behaviors involving withdrawal and/or licking of either hind- and/or forelimbs, but mutants had a higher threshold for pain sensation toward higher temperatures (Figure 4B, a).

Active avoidance test was conducted with a high decibel level noise (120 dB noise) that was used as a source to trigger fear responses in monkeys according to a previous report (Winslow et al., 2002). The mutant monkeys could hear the auditory stimuli (Movie S2), but they covered their ears and hid themselves in the corner of the cage rather than escaping as WT controls did when the noise was presented (Figure 4B, b, Movie S2). These behaviors are very similar to those found in RTT patients with retarded reactions (Neul et al., 2010) or in mouse models (Stearns et al., 2007).

Activity Levels Assessment—Monkeys were under 24-hr continuous monitoring for assessment of activity levels. Compared to WT controls, mutants showed no significantly lower levels of activity during the 24 hr monitoring (WT versus mutant: 19.412 versus 16.522, p = 0.665). During light time (8:00–20:00), no significant difference was observed between mutants and WT controls in levels of activity (mutants versus WT = 30.504 versus 37.920, p = 0.574), and there was also no significant difference in dark time (20:00–8:00) activities (mutants versus WT = 2.542 versus 0.906, p = 0.299) (Figure 4B, c).

Social interaction behaviors were video-recorded and analyzed to assess active interactions. In this test, we found that mutant monkeys exhibited less active social contact, less environmental exploration, but more stereotypical behaviors, compared to WT controls. Moreover, mutant monkeys did not show aggressive behaviors as WT controls did (Figure 4B, d–g; Movies S3 and S4). These results demonstrated stark similarity between mutant monkeys and RTT patients.

Eye-Tracking Patterns

Using primate-unique eye-tracking measures, five mutant female monkeys and five age- and gender-matched WT controls were assessed for social preferences (when presented with monkey faces versus objects) and emotional processing (when presented with monkey faces in different emotional states). Mutant monkeys exhibited a preference for socially weighted stimuli, as they spent more time looking at monkey faces than inanimate objects (Figure 5A; Movie S5). However, when presented faces with aggressive or submissive emotions versus neutral faces, the mutants showed less interest in emotionally charged expressions but preferred neutral faces, as compared with WT monkeys (Figure 5B; Movie S5). These results are consistent with eye-tracking features of RTT patients who show more interest in socially weighted stimuli but have difficulties recognizing emotional expressions (Hetzroni and Rubin, 2006; Djukic and McDermott, 2012).

Transcriptome of Peripheral Blood in *MECP2* Mutant Monkeys and RTT Patients

Due to high-level expression of *MECP2* in neuronal cells, RTT is mainly a nervous system disease. Nevertheless, RTT patients also have many peripheral symptoms including cardiac, pulmonary, muscle, bone, gastro-intestinal, and immune system abnormalities, which may or may not be a direct link to dysfunctions of the nervous system. The peripheral symptoms above could also arise from MeCP2 loss of function in peripheral tissues, because MeCP2 is also expressed in many non-neural cells including fibroblasts. Since peripheral blood from RTT patients is more easily accessible than other tissues, analyses of blood samples for biomarkers may facilitate diagnosis and/or serve as outcome measures for potential clinical interventions. We thus profiled blood transcriptomes of monkeys to uncover potential endophenotype or biomarkers. Through weighted gene coexpression network analyses (WGCNA) (Zhang and Horvath, 2005; Langfelder and Horvath, 2008), we isolated three interconnected gene modules/clusters, which were expressed at different levels between mutant and WT monkeys (Figure 6A). Module-trait correlation matrix demonstrated that these gene clusters were either downregulated (brown and blue modules) or upregulated (turquoise module) in *MECP2* mutant animals with statistical significance (Figure 6B).

Gene ontology (GO) term enrichment of biological process revealed that genes in blue and brown modules were heavily associated with immune responses, which was downregulated in mutant monkeys. This indicates potential deficits in immune functions, which is associated with *MECP2* deficiency. In contrast, genes involved in protein translation and RNA processing (turquoise module) were upregulated in mutants (Figures 6C–6H). To assess the similarity between mutant monkeys and RTT patients, we analyzed the blood transcriptome sequencing in humans from six patients and five healthy age-matched controls. RTT patients' blood samples also revealed modules that were either downregulated and associated with "immune functions" or upregulated and associated with "translation" and "RNA processing" (Figure S4). Moreover, we found a list of genes that showed similar changes in monkeys and human correlated with *MECP2* deficiency (Figures 6I and 6J and S4). These gene expression changes could be potentially used as biomarkers for RTT.

Discussion

RTT is a genetic neurodevelopmental disorder, currently with no cure. A lack of good animal models could potentially contribute to the slow progress of better understandings of the disease and finding cures. Although *MECP2* mutant male mice exhibit phenotypes that resemble some of the symptoms of RTT female patients, it has been difficult or impossible to model more sophisticated disease symptoms in rodents. For example, *Mecp2* knockout rodents show "limb-clasping" phenotype, but this phenotype is shared by neurodegeneration conditions in mice, which is not characteristic for RTT. In contrast, monkey models showed complicated behavioral features, such as fragmented sleep, increased stereotypy, reduced active avoidance of noisy or heat stimuli, and reduced environmental exploration, all of which resemble symptoms of patients. These activities are not widely set up for detection in mouse models.

Some of the characteristics of RTT displayed only in monkey models include male embryonic lethality, social withdrawal, and eye-tracking features, which have never been reported in rodents. Also, MRI of mutant monkeys provided information on longitudinal changes of brain structures with time, which could be very helpful for dissecting mechanisms of RTT. Although it is difficult to use MRI in clinical settings to track early-stage neurodevelopmental changes in patients, limited human RTT patient MRI data showed striking similarity with the monkey data and further attest to the validity of our monkey models. Obviously, longitudinal MRI studies in rodents will be close to impossible, and, even if they are done, the short lifespan and rapid brain development of rodents as well as dramatic differences in brain structures between human and rodents will potentially make rodent models even less compelling. Moreover, in peripheral blood transcriptome sequencing, the genetic changes of monkey models overlap with that of RTT patients, which could be important molecular indicators to reflect RTT.

This work is also different from a previous report on monkey models of *MECP2* duplication syndrome (Liu et al., 2016). In that report, monkeys with overexpressed *MECP2* were generated via virus-induced gain-of-function expression of exogenous *MECP2*, which shares little similarity in terms of disease mechanisms with RTT. The ectopic pan-neuronal expression of *MECP2* transgene may generate ectopic phenotypes, which are different from clinical *MECP2* duplication mutations, where increased *MECP2* expression only happens in neurons that originally express the gene, as not all neurons express *MECP2. MECP2* mutant monkeys in our case were generated through TALEN-mediated gene editing that induced *MECP2* deficiency, which is believed to be direct cause for RTT and thus making it possible to study the disease mechanism.

Great progress in neuroscience has been made and will continue by studying rodents and other simpler species, or even directly by clinical cases. NHP research will surely not replace these approaches and should be considered only in cases in which monkeys are the best and only available models for research. It seems RTT is a typical case in which monkey models may serve as a great system to study the mechanism and progression of the disease and to deliver new and effective treatments, since brains of other species are just too dissimilar to human brains. Non-primate models certainly are not able to mimic the

sophisticated features of cognition, social interactions, etc. Our study showed that a valid monkey model might offer robust phenotype or endophenotype, which could be implemented as outcome measures in human clinical trials in the future to facilitate drug development.

Star★Methods

Detailed methods are provided in the online version of this paper and include the following:

Contact for Reagent and Resource Sharing

Further information and requests for reagents may be directed to and will be fulfilled by the Lead Contact, Yongchang Chen (chenyc@lpbr.cn).

Experimental Model and Subject Details

Monkey Studies—The cynomolgus monkey (*Macaca fascicularis*) facility in this study is accredited by AAALAC International and all experimental protocols were approved in advance by the Institutional Animal Care and Use Committee of Yunnan Key Laboratory of Primate Biomedical Research. The animals were housed in a controlled environment (temperature: $22 \pm 1°C$; humidity: 50% ±5% RH) with 12 hr light/ 12 hr dark cycle (lights on at 08:00 a.m.). All animals were given commercial monkey diet twice a day with tap water ad libitum and were fed fruits and vegetables once daily. During and after experiments, monkeys have been under careful veterinary oversight to ensure good health. They were never involved in previous procedures, and are drug and/or test naive.

Human Studies—Human subject research was approved by Department of Pediatrics at Peking University First Hospital. Subjects' written informed consent was obtained prior to any study procedures. Subject details can be found in Table S4.

Method Details

Generation of TALEN Induced MECP2 Knockout Cynomolgus Monkeys—
Procedures for superovulation, oocytes collection, intracytoplasmic sperm injection (ICSI), TALENs injection, and embryo transfer and pregnancy diagnosis are in accordance with previous report (Liu et al., 2014). In brief, thirty female cynomolgus monkeys aged 5-10 with regular menstrual cycles were selected as oocyte donors for superovulation, which were intramuscular injected with rhFSH (Recombinant Human FSH, Gonal F, Laboratories Serono) for 8 days and then with rhCG (Recombinant Human Chorionic Gonadotropin alpha for Injection, Merck Serono) on day 9. Oocytes were collected by laparoscopic follicular aspiration (STORZ) 32-35 hr after rhCG administration. Mature oocytes were used to perform ICSI. After co-incubation of oocytes and spermatozoa for 8-10 hr, fertilization was confirmed for the presence of two pronuclei and two polar bodies. About 5 pl of 2 ng/ml TALEN-coding plasmids were mixed and injected in the cytoplasm of fertilized oocytes. Injected embryos were cultured in chemically defined protein-free hamster embryo culture medium-9 (HECM-9, Millipore) containing 10% fetal bovine serum (FBS, GIBCO) at 37°C in 5% CO_2 to allow embryo development. The quality cleaved embryos at 2-cell to blastocyst were transferred into the oviduct of the matched recipient monkeys. Fourty-one

females were used as surrogate recipients for TALENs injected embryos, and typically, 2-3 embryos were transferred for each transfer. The earliest pregnancies were diagnosed by ultrasonography about 20 days after embryo transfer. Aborted tissues of all available parts of body were collected and then either fixed in 4% Paraformaldehyde (PFA, Sigma-Aldrich) or quick frozen in liquid nitrogen and stored at −80°C. All live neonatal baby monkeys were fed by host mothers or nurtured manually.

Genomic Mutations Analyses—Tissues including placenta, umbilical cord, ear skin fibroblasts, peripheral blood were collected and digested in lysis buffer (10 μM Tris-HCl, 0.4 M NaCl, 2 μM EDTA, 1% SDS and 100 μg/ml Proteinase K). The genomic DNA was extracted from lysate by phenol-chloroform recovered by alcohol precipitation. Genomic mutations of miscarried and live monkeys were identified by T7EN1 cleavage assay with T7 Endonuclease (NEB) and Sanger sequencing as described previously (Liu et al., 2014). Age- and gender-matched WT controls were housed and fed together with mutants under the same ambient condition. PCR products with mutations detected by T7EN1 cleavage assay were sub-cloned into T vector (Takara). For each sample, colonies were picked up randomly and Sanger sequenced by M13-47 primer.

Off-targets Assay—The potential off-target sites were predicted using a genome-wide TALEN target site prediction tool named TALENoffer (Grau et al., 2013; Liu et al., 2014). The statistical model of TALENoffer assumes that the possible nucleotides on a target site can be traced from the repeat-variable di-residue of the corresponding repeat, which determines DNA binding specificity. Using a definite cutoff (TALENoffer score > −1.8) to define potential off-targets in the whole genome, a total of 41 exonic loci were predicted to be potential off-target sites. The fragments of all the potential off-target loci from 3 pairs of TALENs were PCR amplified, then subjected to Sanger sequencing.

Western Blotting—For western blotting analysis, fibroblasts from ear, brain, and placenta tissues were lysed, of which MeCP2 protein expression analyzed using GAPDH as an internal control for protein were loading. About 40 μg of lysate was mixed with 5 × loading buffer, boiled for 5 min and loaded onto 10% SDS-PAGE gels and transferred onto a PVDF membrane (Millipore). The membranes were blocked with 5% non-fat milk for 1 hr, and then incubated with primary antibodies (MeCP2, Cell Signaling Technology; GAPDH, Kangcheng) overnight at 4°C and subsequently for 1 hr at room temperature (25°C) with Goat Anti-Rabbit IgG Antibody, (H+L) HRP conjugate (Millipore) or Goat anti-Mouse IgG, (H+L) HRP conjugate (Millipore). The epitope was tested using Pierce ECL Western Blotting Substrate (Thermo Scientific).

MRI Scanning—Monkeys at three different stages (4 mutants at 8 months, 3 mutants at 15 months and 20 months) were arranged for MRI analysis. In each stage, more than 10 age- and gender-matched WT monkeys (11 WT at 8 months, 12 WT at 15 months, and 11 WT at 20 months) were included in the test. MR images were scanned using a Philips 3.0 Tesla MRI scanner. Before the scan, all animals were pre-anesthetized intramuscularly with ketamine hydrochloride (15 mg/kg; Gutian, China) and xylazine (1.5 mg/kg; Huamu, China). The sagittal 3D T1-weighted images were acquired using an inversion-recovery

prepared 3-D spoiled gradient echo (SPGR) pulse sequence. To quantitatively measure the brains of mutant and WT monkeys, T1-weighted MR images were processed in a double-blind manner using an in-house developed computational pipeline. Specifically, all T1-weighted images were skull-stripped, corrected for intensity in homogeneity and resampled to be an isotropic resolution (0.375 mm × 0.375 mm × 0.375 mm). Then, tissue segmentation of T1-weighted images into gray matter (GM), white matter (WM), and cerebrospinal fluid (CSF) was performed by a machine learning-based method, which is a state-of-the-art method for segmentation of the challenging developing brain (Wang et al., 2015). After tissue segmentation, the non-cortical structures were masked and filled, and each brain was separated into left and right hemispheres. Next, for each hemisphere of each image, the inner cortical surface (GM-WM interface) and outer cortical surface (GM-CSF interface) were reconstructed by using a topology-preserving deformable surface method (Li et al., 2014). The cortical thickness of each cortical vertex was computed as the average value of the minimum distance from inner to outer surfaces and the minimum distance from outer to inner surfaces. The surface area of each vertex was computed as one-third the sum of areas of all triangles associated with that vertex on the central surface, which is the geometric average of the inner and outer surfaces. To parcellate the cortical regions of each image, the INIA19 template was nonlinearly aligned onto each image using diffeomorphic demons based on the tissue maps, and accordingly its corresponding cortical label map was propagated onto each image and its corresponding cortical surfaces. As the INIA19 template (Rohlfing et al., 2012) contains too many tiny regions in sub-cortex and white matter, which will lead to inaccurate measurements, to parcellate the sub-cortex and whiter matter into relatively large regions for each image, the UNC Primate Brain Atlas was nonlinearly aligned onto each image using diffeomorphic demons (Vercauteren et al., 2009) based on the tissue maps, and then its corresponding subcortical and white matter labels were propagated onto each image. For global measurement, the total GM volume, total WM volume, total cortical GM volume, total cortical surface area and average cortical thickness were computed for each image. For regional measurement, a total of 60 subregions of each monkey's brain was segmented and analyzed, the cortical volume, cortical surface area and average cortical thickness were computed for each cortical region. Note that cortical thickness and surface area, which jointly determine the cortical volume, has distinct biological mechanism and developmental patterns, thus allowing us better understanding the cortical changes in mutant monkeys. And the volume of each subcortical region and each WM region were also computed.

EKG Recording—The monkeys were randomized in a double-blind manner to obtain the EKG signals by SYMTOP biophysical recording system (UEA-41FZ, Symtop Instrument, China) with a sample rate of 1000 Hz. The standard 12-lead EKG was monitored and recorded for over 10 min on awake monkeys with spontaneous breathing. The heart rate (HR) and QT interval (QTc) were measured automatically. Corrected QTc was measured using the Bazett's correction formula (QTc = QT/SQRT (RR)) (Shah, 2002).

Sleep Pattern—Behaviors of 10 cynomolgus monkeys, including 5 mutants and 5 WT controls, were continuously video-recorded for 3 consecutive nights from 19:00 p.m. to 9:00 a.m. The video system consists of 10 infrared video cameras and a hard disk video recorder.

One camera faces one cage, ensuring that the entire cage was visible. Behaviors were scored by three raters independently who were blind to the experimental design. Three behavioral states, awake, transitional and relaxed sleep were scored in 1 min epochs (Noser et al., 2003). States lasting < 30 s were not considered, whereas states lasting between 30 and 59 s were rounded to 1 min. The animals were considered to be awake when locomotion occurred, or when over 3 times of body or limb movement occurred within 1 min while in sitting or lying position. Sleep was scored as transitional when 1 or 2 times of body or limb movement occurred within 1 min while in sitting position. During relaxed sleep, the animals always kept the head below the shoulders or bent backward with no body or limb movements when sitting. Relaxed sleep was also scored when the animal was lying immobile. Sleep duration consisted of all 1 min epochs scored as transitional or relaxed sleep. Sleep fragmentation was defined as the frequency of waking bouts lasting 1 min or longer per night.

Pain Threshold Test—An improved hot-plate method (Winslow et al., 2002) was used to determine differences in pain threshold between 5 *MECP2* mutants and 5 WT monkeys. The method using slowly increasing thermal stimulus applied mostly to the skin of animal plantar surface (Alshahrani et al., 2012). The equipment consists of several components, including an aluminum plate (40 cm × 40 cm) with the heating system underneath and a Plexiglas observation chamber above (40 cm × 40 cm × 80 cm), one heat controlling unit, one video camera for behaviors recording and one foot switch for remote control of the unit. The aluminum plate is divided into four equal parts (10 cm × 10 cm) and each part has a thermometer in the center. Before testing, visually inspect the equipment to corroborate the chosen heating rates (e.g., 6°C /min), initial standby and final cut-off temperatures (e.g., 25°C and 55°C, respectively). Afterward, the experimenters felt the equipment themselves. Withdraw the hand from the hot plate at the moment of pain perception. The temperature should not cause harm to the skin nor produce any later discomfort. Once the equipment is ready, the monkeys were gently placed into the Plexiglass observation chamber, which was on top of the heating plate. Each monkey was given 5 min to acclimate to the equipment. Once the animal felt comfortable in the observation chamber, the plate was heated by pressing the footswitch. When the monkey exhibited nocifensive behaviors involving withdrawal and/or licking of either hind- and/or fore-limb, the temperature was recorded according to the thermometer in which the monkey stayed. Each monkey was tested once daily at the same time of the day for 3 test sessions.

Active Avoidance Test—A modified version of active avoidance test was used to evaluate monkeys' fear responses to loud noise according to previously report (Winslow et al., 2002). The equipment consists of several components, which included two adjoining Plexiglas observation chambers (80 cm × 80 cm × 80 cm) connected by a tunnel (60 cm × 40 cm × 20 cm), two high-pitch loudspeakers, a video camera for recording behaviors and a foot switch for remote control of the loudspeaker. Each monkey was tested once daily at the same time of the day for 3 test sessions, and the time spent escaping from the noise was recorded. During the test, each monkey was carried from the home cage in a transport cage, which was placed at the door of the chamber. The door was then opened and the monkey entered the chamber. Each monkey was given a maximum of 5 min to enter themselves

otherwise they were pushed into the chamber. Each monkey had 5 min to adapt to the chamber and learn to shuttle between two chambers. Then loud noises (120 dB) were presented in the chamber where monkeys stayed according to previous studies (Winslow et al., 2002). This would cause monkeys to either escape to the adjoining chamber or crouch in the start chamber covering their ears. The noise was stopped when the monkeys escaped to the other chamber. In order not to inflict harm to monkeys, the noise should not exceed 5 min. The monkeys' responses to noise stimuli and the time spent to escape were analyzed.

Activity Levels Assessment—The Actical Physical Activity Monitors (Respironics, Pennsylvania, USA) used to monitor activity levels of free-moving monkeys (five mutant females and five age-matched WT females) are water resistant (IEC Standard 60529 IPX7), lightweight (16 g), and small (2.9 cm × 3.7 cm × 1.1 cm). The Actical monitor uses a single internal omni-directional accelerometer that senses motion in all direction, integrates the amplitude and frequency of detected motion and produces an electrical current varying in magnitude. Therefore, an increased intensity of motion produces an increase in voltage. Actical stores the information in the form of activity counts. Monkeys' ID, body weight and length information were put into the Actical (Software version 3.1.0) before test. The device was placed on the monkeys' waists with soft belts. The monitor was mounted in the same waist position in each monkey to ensure the consistency of obtained data. The activity data were collected at a sampling rate of 32 HZ and in epochs as short as 1 s. Each monkey was monitored for 3 days. Data were downloaded using the Actireader that was connected to the PC via an RS-232 serial cable, and was communicated with Actical devices using a short range telemetric link.

Social Interaction Test—The social interaction test is a simple test in which behaviors are video-recorded and analyzed to assess social deficits in mutant monkeys with their age- and gender- matched control monkeys. The measured behaviors include active social contact, environmental exploration, stereotypical behaviors, and aggressive behaviors. Active social contact is defined as initiating a play, sharing toys, grooming for others, sitting together (within another monkey's arms' reach or in contact), etc. Environmental exploration includes tactile exploration of the cage or environment and oral exploration of the cage or environment (Altmann, 1974). The stereotypical behaviors are defined as repetitive and consistent actions with no apparent purposes, including pacing (repetitive, ritualized movement usually involving circling the cage), digit sucking (sucking on a finger or toe), self-grasping (grabbing or holding onto part of their own body), rocking (a back and forth movement of the upper body with still feet), bouncing (jumping up and down on all four legs), cage shaking (any vigorous shaking of the cage), body spasms (a quick shake of the body), and lip-smacking (pursing the lips together and moving them to produce a smacking sound) (Altmann, 1974). Aggressive behaviors included a bite, slap, grab, stare threat, open-mouth threat, chase, and forced displacement (Qin et al., 2015). Each monkey was recorded once daily at the same time (9:00-10:00) of the day for 3 test sessions. The recordings were simultaneously analyzed by 3 viewers using a standardized behavioral classification.

Eye Tracking—Eye tracking is a useful technique in assessing cognitive changes in Rett syndrome, and we used a Tobii Pro TX300 Eye Tracker (Tobii Technology AB, Danderyd,

Sweden) in this study. Eye tracking data were sampled at 300 Hz and shown on a 23-inch monitor (with a resolution of 1920 × 1080 pixels) (Simpson et al., 2016). Five mutant monkeys and 5 age- and gender-matched WT monkeys were included in this task. The monkeys were trained habituating themselves to sit in the primate chair and to restrict the head movement by a helmet that was made of high density Ethylene-vinyl acetate (EVA). The helmets were customized to fit with each monkey's head. Once the monkeys were acclimated to the experimental procedure, two consecutive tests including paired face-object preference test and paired emotional faces preference test (Figure 4A), were conducted with an interval of about one week. During the tests, the eye tracker was set in front of the monkeys, with a distance of about 69 cm away from the monkeys' eyes, and ambient light levels were reduced to diminish distraction. As the monkeys were relatively quiet in their adolescence, the water was not restricted in completing looking tasks with the consideration of animal welfare. We studied the monkeys' free viewing behavior, which represents an innate behavior and potentially better reflects the monkeys' social and emotional information processing functions. Before each test, each monkey was calibrated to Tobii Studio's two preset locations, and the audio cartoon symbols were also used as calibration points to attract the monkeys' attention. During paired face-object preference tests, 20 stimuli were presented to each monkey. Each stimulus consists of a monkey's neutral face and an object, which is familiar to the monkeys. Ten faces (from 7 monkeys) and 10 different objects composed the 20 stimuli with counterbalanced location. Faces and objects were about $8.5 \times 9°$ of visual angle and separated by 8.5°. During paired emotional faces preference test, 14 stimuli were presented to each monkey. Each stimulus composed of a pair of faces of the same monkey. The total stimuli consisted of 5 different monkeys, each posing two or three expressions. These expressions included 3 kinds of emotional stimuli: neutral-aggression, neutral-submission and aggression- submission, which were presented with counterbalanced sequence. Stimuli were presented using Tobii Studio software (Tobii Technology AB, Danderyd, Sweden) and eye tracking data were sampled at 300 Hz. The monkey faces were chosen from PrimFace database (website: https://visiome.neuroinf.jp/primface). The left part and the right part of each stimulus, separated by the midline of the screen, are simply defined as two AOIs (area of interests), which represents the corresponding faces or objects. Looking counts and looking duration of different AOIs were summarized automatically by Tobii Studio software.

Peripheral Blood Collection, Library Preparation, Sequencing and WGCNA—
All six Chinese patients with Rett syndrome and five healthy children were recruited in 2015 and 2016. All the patients were interviewed and diagnosed according to clinic diagnostic criteria and mutations of *MECP2*. A questionnaire including clinical manifestation, family reproductive history, etc. was filled by the parents after signing an informed consent. Ethical approval was obtained from Clinical Research Ethics Committee, Peking University First Hospital. Genomic DNA was extracted using standard methods from the peripheral blood leukocytes of RTT patients and their parents. *MECP2* mutational analysis was performed using polymerase chain reaction (PCR). If no mutations were identified, the MLPA-P015 probe (SALSA MLPA kit P015MECP2, MRC-Holland, Amsterdam, Holland) was used to detect large deletions or duplications. MLPA products were separated and analyzed using the ABI Prism 3100 Genetic Analyzer and Genescan software according to manufacturer's

recommendations. For human patients (5 healthy and 6 RTT) and monkeys (5 mutant and 9 WT), peripheral blood of mutants and controls were collected intravenously. Globin transcripts were first depleted from total RNA using the GLOBINclear kit (Life Technologies) following the manufacturer's protocols. All sequenced libraries were prepared using the TruSeq RNA Library Prep Kit v2 (Illumina) and sequencing data were mapped to either human genome (Ensembl GRCh38.79) or monkey genome (Ensembl Mmul_1.79) using TopHat (v.2.0.12). A signed network was constructed using all genes that were differentially expressed between WT and mutant blood samples at a cutoff of log2 (FPKM) differences at 0.1 or higher. Soft power parameter was estimated and used to derive a pairwise distance matrix for selected genes using the topological overlap measure, and the dynamic hybrid cut method was used to detect clusters. The node centrality, defined as the sum of within-cluster connectivity measures, was used to rank genes for "hub-ness" within each cluster. Hub genes in each module were graphically depicted using VisANT 1.0.

Statistical Analyses—Data analysis was conducted using the SPSS version 19.0 software package (SPSS, Chicago, IL, USA). Western blotting image data were processed with ImageJ software. The normality of the behavioral data were analyzed by Kolmogorov-Smirnov test. All the behavioral data (Kolmogorov-Smirnov tests: $p > 0.05$), except active avoidance behavior, environmental exploration, stereotypical behaviors and aggressive displays were normally distributed. One-way ANOVA was used to analyze the differences between mutant monkeys and WT monkeys in sleep pattern, pain threshold, and active social contact, and Wilcoxon's signed rank tests were used to analyze the active avoidance behavior, environmental exploration, stereotypical behaviors and aggressive displays. The measures of looking counts and looking duration were obtained from eye-tracking paradigm. The normality of eye tracking data were analyzed by Kolmogorov-Smirnov test, and they were normally distributed ($p > 0.05$). In the paired face-object preference test, the counts and duration of looking at monkey faces versus objects were determined and analyzed with one-way ANOVA, and in the test of paired emotional faces preference, they were also evaluated with one-way ANOVA to compare mutant monkeys with WT monkeys. The interactions were further analyzed with two-way ANOVA. The normality of data for monkeys' growth and development, including body weight, head circumference, body length, and biparietal diameter, were also analyzed by Kolmogorov-Smirnov test, the results of which demonstrate that they were normally distributed ($p > 0.05$). And the data were further analyzed in separate 2 (groups: mutant versus WT) × 5 (time: 6 months, 9 months, 12 months, 15 months and 18 months) repeated-measures ANOVAs, with time being the repeated-measure. The measurements of each region were analyzed by Rank Sum test, and multiple comparisons were performed with the false discovery rate (FDR) correction (Benjamini and Hochberg, 1995). The normality of data for heart rate and electrocardiogram were analyzed by Kolmogorov-Smirnov test ($p > 0.05$), and one-way ANOVA was used to compare mutant monkeys with WT monkeys. The alpha level was set at $p = 0.05$ and all p values were generated using two-sided tests. All data are presented as the mean ± SEM.

Data and Software Availability

For material sharing, monkeys' materials (such as blood, mRNA, or DNAs) are available and free for sharing. However, as for patients, samples in the study were limited and there are

few left for sharing. Further information and requests for raw data, analysis details, and DNA/RNA samples can be directed to and fulfilled in compliance with IACUC protocol requirements by Lead Contact Yongchang Chen (chenyc@lpbr.cn). The RNA-seq raw data for monkeys and patients can be shared freely, and have been deposited in a public repository and the accession numbers are listed as below.

The accession numbers for the RNA-seq data reported in this paper are in the Sequence Read Archive (SRA) database at the NCBI (SRA: SRP105312 and SRP105313). The RNA-seq raw data of children reported in this paper have been deposited to the NCBI (SRA: SRP105312) (https://www.ncbi.nlm.nih.gov/Traces/study/?acc=SRP105312). The RNA-seq raw data of cynomolgus monkeys have been deposited to the NCBI (SRA: SRP105313) (https://www.ncbi.nlm.nih.gov/Traces/study/?acc=SRP105313).

Supplementary Material

Refer to Web version on PubMed Central for supplementary material.

Acknowledgments

References

Alshahrani, S., Fernandez-Conti, F., Araujo, A., DiFulvio, M. Rapid determination of the thermal nociceptive threshold in diabetic rats. J Vis Exp. 2012. Published online May 17, 2012. http://dx.doi.org/10.3791/3785

Altmann J. Observational study of behavior: Sampling methods. Behaviour. 1974; 49:227–267. [PubMed: 4597405]

Amir RE, Van den Veyver IB, Wan M, Tran CQ, Francke U, Zoghbi HY. Rett syndrome is caused by mutations in X-linked MECP2, encoding methyl-CpG-binding protein 2. Nat Genet. 1999; 23:185–188. [PubMed: 10508514]

Benjamini Y, Hochberg Y. Controlling the false discovery rate: A practical and powerful approach to multiple testing. J R Stat Soc Ser A Stat Soc. 1995; 57:289–300.

Bjure J, Uvebrant P, Vestergren E, Hagberg B. Regional cerebral blood flow abnormalities in Rett syndrome. Eur Child Adolesc Psychiatry. 1997; 6(Suppl 1):64–66. [PubMed: 9452923]

Carter JC, Lanham DC, Pham D, Bibat G, Naidu S, Kaufmann WE. Selective cerebral volume reduction in Rett syndrome: A multiple-approach MR imaging study. AJNR Am J Neuroradiol. 2008; 29:436–441. [PubMed: 18065507]

Chen RZ, Akbarian S, Tudor M, Jaenisch R. Deficiency of methyl-CpG binding protein-2 in CNS neurons results in a Rett-like phenotype in mice. Nat Genet. 2001; 27:327–331. [PubMed: 11242118]

Djukic A, McDermott MV. Social preferences in Rett syndrome. Pediatr Neurol. 2012; 46:240–242. [PubMed: 22490770]

Glaze DG. Rett syndrome: Ofgirls and mice—lessons for regression in autism. Ment Retard Dev Disabil Res Rev. 2004; 10:154–158. [PubMed: 15362175]

Grau J, Boch J, Posch S. TALENoffer: Genome-wide TALEN off-target prediction. Bioinformatics. 2013; 29:2931–2932. [PubMed: 23995255]

Guy J, Hendrich B, Holmes M, Martin JE, Bird A. A mouse Mecp2-null mutation causes neurological symptoms that mimic Rett syndrome. Nat Genet. 2001; 27:322–326. [PubMed: 11242117]

Hagberg B, Aicardi J, Dias K, Ramos O. A progressive syndrome of autism, dementia, ataxia, and loss of purposeful hand use in girls: Rett's syndrome: report of 35 cases. Ann Neurol. 1983; 14:471–479. [PubMed: 6638958]

Hagberg, B., Hanefeld, F., Percy, A., Skjeldal, O. An updateon clinically applicable diagnostic criteria in Rett syndrome. Eur J Paediatr Neurol; Comments to Rett Syndrome Clinical Criteria Consensus Panel Satellite to European Paediatric Neurology Society Meeting; Baden Baden, Germany. 11 September 2001; 2002. p. 293-297.

Hetzroni OE, Rubin C. Identifying patterns of communicative behaviors in girls with Rett syndrome. Augment Altern Commun. 2006; 22:48–61. [PubMed: 17114158]

Izpisua Belmonte JC, Callaway EM, Caddick SJ, Churchland P, Feng G, Homanics GE, Lee KF, Leopold DA, Miller CT, Mitchell JF, et al. Brains, genes, and primates. Neuron. 2015; 86:617–631. [PubMed: 25950631]

Jennings CG, Landman R, Zhou Y, Sharma J, Hyman J, Movshon JA, Qiu Z, Roberts AC, Roe AW, Wang X, et al. Opportunities and challenges in modeling human brain disorders in transgenic primates. Nat Neurosci. 2016; 19:1123–1130. [PubMed: 27571191]

Katz DM, Bird A, Coenraads M, Gray SJ, Menon DU, Philpot BD, Tarquinio DC. Rett syndrome: Crossing the threshold to clinical translation. Trends Neurosci. 2016; 39:100–113. [PubMed: 26830113]

Langfelder P, Horvath S. WGCNA: An R package for weighted correlation network analysis. BMC Bioinformatics. 2008; 9:559. [PubMed: 19114008]

Li G, Nie J, Wang L, Shi F, Gilmore JH, Lin W, Shen D. Measuring the dynamic longitudinal cortex development in infants by reconstruction of temporally consistent cortical surfaces. Neuroimage. 2014; 90:266–279. [PubMed: 24374075]

Li Q, Loh DH, Kudo T, Truong D, Derakhshesh M, Kaswan ZM, Ghiani CA, Tsoa R, Cheng Y, Sun YE, Colwell CS. Circadian rhythm disruption in a mouse model of Rett syndrome circadian disruption in RTT. Neurobiol Dis. 2015; 77:155–164. [PubMed: 25779967]

Liu H, Chen Y, Niu Y, Zhang K, Kang Y, Ge W, Liu X, Zhao E, Wang C, Lin S, et al. TALEN-mediated gene mutagenesis inrhesus and cynomolgus monkeys. Cell Stem Cell. 2014; 14:323–328. [PubMed: 24529597]

Liu Z, Li X, Zhang JT, Cai YJ, Cheng TL, Cheng C, Wang Y, Zhang CC, Nie YH, Chen ZF, et al. Autism-like behaviours and germline transmission in transgenic monkeys overexpressing MeCP2. Nature. 2016; 530:98–102. [PubMed: 26808898]

Lombardi LM, Baker SA, Zoghbi HY. MECP2 disorders: From the clinic to mice and back. J Clin Invest. 2015; 125:2914–2923. [PubMed: 26237041]

Naidu S, Kaufmann WE, Abrams MT, Pearlson GD, Lanham DC, Fredericksen KA, Barker PB, Horska A, Golay X, Mori S, et al. Neuroimaging studies in Rett syndrome. Brain Dev. 2001; 23(Suppl 1):S62–S71. [PubMed: 11738844]

Neul JL, Kaufmann WE, Glaze DG, Christodoulou J, Clarke AJ, Bahi-Buisson N, Leonard H, Bailey ME, Schanen NC, Zappella M, et al. Rett syndrome: Revised diagnostic criteria and nomenclature. Ann Neurol. 2010; 68:944–950. [PubMed: 21154482]

Noser R, Gygax L, Tobler I. Sleep and social status in captive gelada baboons (Theropithecus gelada). Behav Brain Res. 2003; 147:9–15. [PubMed: 14659565]

Patterson KC, Hawkins VE, Arps KM, Mulkey DK, Olsen ML. MeCP2 deficiency results in robust Rett-like behavioural and motor deficits in male and female rats. Hum Mol Genet. 2016; 25:3303–3320. [PubMed: 27329765]

Qin D, Rizak J, Feng X, Yang S, Yang L, Fan X, Lü L, Chen L, Hu X. Cortisol responses to chronic stress in adult macaques: Moderation by a polymorphism in the serotonin transporter gene. Behav Brain Res. 2015; 278:280–285. [PubMed: 25311283]

Reiss AL, Faruque F, Naidu S, Abrams M, Beaty T, Bryan RN, Moser H. Neuroanatomy of Rett syndrome: A volumetric imaging study. Ann Neurol. 1993; 34:227–234. [PubMed: 8338347]

Rett A. On a unusual brain atrophy syndrome in hyperammonemia in childhood. Wien Med Wochenschr. 1966; 116:723–726. [PubMed: 5300597]

Ricceri L, De Filippis B, Laviola G. Mouse models of Rett syndrome: From behavioural phenotyping to preclinical evaluation of new therapeutic approaches. Behav Pharmacol. 2008; 19:501–517. [PubMed: 18690105]

Rohlfing T, Kroenke CD, Sullivan EV, Dubach MF, Bowden DM, Grant KA, Pfefferbaum A. The INIA19 template and NeuroMaps atlas for primate brain image parcellation and spatial normalization. Front Neuroinform. 2012; 6:27. [PubMed: 23230398]

Schanen NC, Kurczynski TW, Brunelle D, Woodcock MM, Dure LS 4th, Percy AK. Neonatal encephalopathy in two boys in families with recurrent Rett syndrome. J Child Neurol. 1998; 13:229–231. [PubMed: 9620015]

Shah RR. The significance of QT interval in drug development. Br J Clin Pharmacol. 2002; 54:188–202. [PubMed: 12207642]

Shultz S, Opie C, Atkinson QD. Stepwise evolution of stable sociality in primates. Nature. 2011; 479:219–222. [PubMed: 22071768]

Simpson EA, Nicolini Y, Shetler M, Suomi SJ, Ferrari PF, Paukner A. Experience-independent sex differences in newborn macaques: Females are more social than males. Sci Rep. 2016; 6:19669. [PubMed: 26794858]

Stearns NA, Schaevitz LR, Bowling H, Nag N, Berger UV, Berger-Sweeney J. Behavioral and anatomical abnormalities in Mecp2 mutant mice: A model for Rett syndrome. Neuroscience. 2007; 146:907–921. [PubMed: 17383101]

Subramaniam B, Naidu S, Reiss AL. Neuroanatomyin Rett syndrome: Cerebral cortex and posterior fossa. Neurology. 1997; 48:399–407. [PubMed: 9040729]

Trapnell C, Pachter L, Salzberg SL. TopHat: discovering splice junctions with RNA-Seq. Bioinformatics. 2009; 25:1105–1111. [PubMed: 19289445]

Veeraragavan S, Wan YW, Connolly DR, Hamilton SM, Ward CS, Soriano S, Pitcher MR, McGraw CM, Huang SG, Green JR, et al. Loss of MeCP2inthe rat models regression, impaired sociability and transcriptional deficits of Rett syndrome. Hum Mol Genet. 2016; 25:3284–3302. [PubMed: 27365498]

Vercauteren T, Pennec X, Perchant A, Ayache N. Diffeomorphic demons: Efficient non-parametric image registration. Neuroimage. 2009; 45(1, Suppl):S61–S72. [PubMed: 19041946]

Wang L, Gao Y, Shi F, Li G, Gilmore JH, Lin W, Shen D. LINKS: Learning-based multi-source IntegratioN frameworK for Segmentation of infant brain images. Neuroimage. 2015; 108:160–172. [PubMed: 25541188]

Winslow JT, Parr LA, Davis M. Acoustic startle, prepulse inhibition, and fear-potentiated startle measured in rhesus monkeys. Biol Psychiatry. 2002; 51:859–866. [PubMed: 12022958]

Yang H, Wang H, Shivalila CS, Cheng AW, Shi L, Jaenisch R. One-step generation of mice carrying reporter and conditional alleles by CRISPR/Cas-mediated genome engineering. Cell. 2013; 154:1370–1379. [PubMed: 23992847]

Zhang B, Horvath S. A general framework for weighted gene co-expression network analysis. Stat Appl Genet Mol Biol. 2005; 4:Article 17.

Highlights

- Modeling Rett syndrome using TALEN-edited MECP2 mutant cynomolgus monkeys

- MECP2 mutations induce male lethality and females resembling RTT patients

- Phenotypes include brain developmental and complex behavioral abnormalities

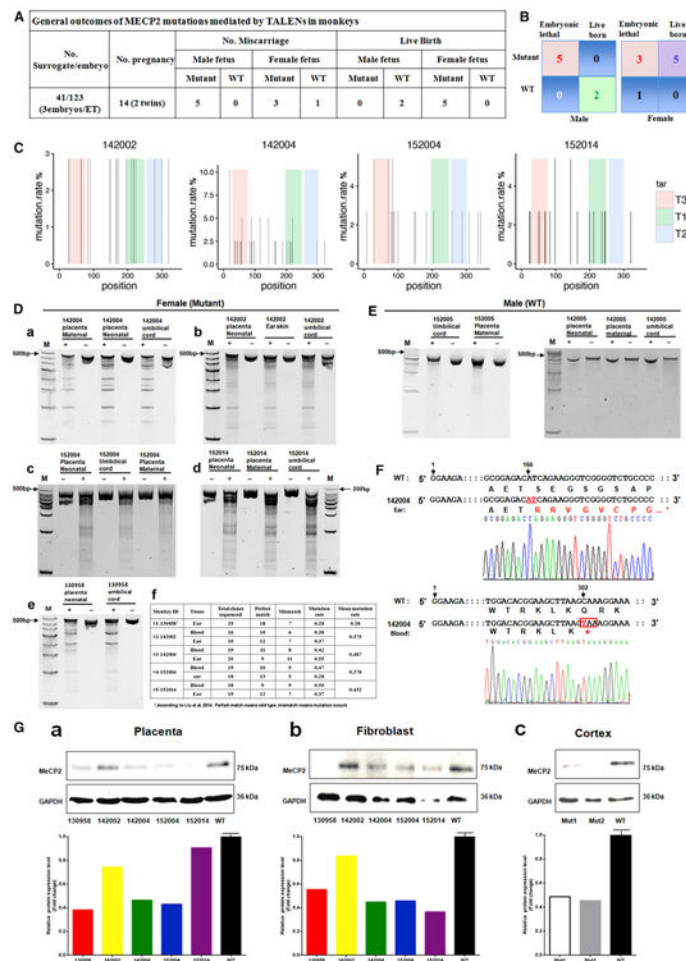- The model will facilitate the deciphering of RTT mechanisms and development of new interventions

Figure 1. Generation of *MECP2* Mutant Cynomolgus Monkeys via TALENs

(A) General outcomes of MECP2 mutations mediated by TALENS in monkeys.

(B) Conclusion of mutant and WT monkeys including alive founders and aborted fetuses.

(C) Sanger sequencing in placenta, skin, and umbilical cord indicated there were multiple mutations on exon 3 of *MECP2* gene. All detected point mutations were plotted based on their positions and mutation rates in the entire 351 bp on exon 3. See also Table S2.

(D) T7EN1 cleavage analysis and mutations of the placenta and skin tissue of five alive female monkeys. Mutation rates of five female monkeys calculated from Sanger sequencing on exon 3 of *MECP2* (a–e). From total clones sequenced, perfect match (WT) and mismatch (mutant) sequences were identified comparing with reference sequences and counted for calculating mutation rates (f). For more mutant information, see also Tables S1 and S2.

(E) T7EN1 cleavage analysis and mutations of the placenta and skin tissue of two alive male monkeys.

(F) Sanger sequencing further identified that the mutations happened at the targeted exon in an alive monkey's ear skin and blood.

(G) Comparison of protein levels between the mutants and WT controls via western blots. (a and b) Western blots and statistical analysis of MeCP2 protein expressions in lysate of placenta (a) and skin fibroblasts (b) from alive mutant monkeys and WT controls; (c) western blots and statistical analysis of cortices from aborted WT and mutant fetuses.

Western blot image data were averaged from five repeats with ImageJ software. Compared with WT monkeys (n = 3, relativeMeCP2 value is set as 100%), all of the mutant monkeys exhibited lower MeCP2 protein expression. For MeCP2 expression levels in placenta of monkeys #130958, 142002, 142004, 152004, and 152014 were 44.71%, 16.47%, 55.26%, 54.28%, and 63.57%, respectively, lower than those in WT; in fibroblasts, the numbers were 61.92%, 25.79%, 53.63%, 57.10%, and 9.46%, lower than WT. In the cortices, male monkeys Mut1 and Mut2 expressed MeCP2 at levels 51.36% and 54.74%, respectively, lower than WT (n = 3, relative MeCP2 value is set as 100%).
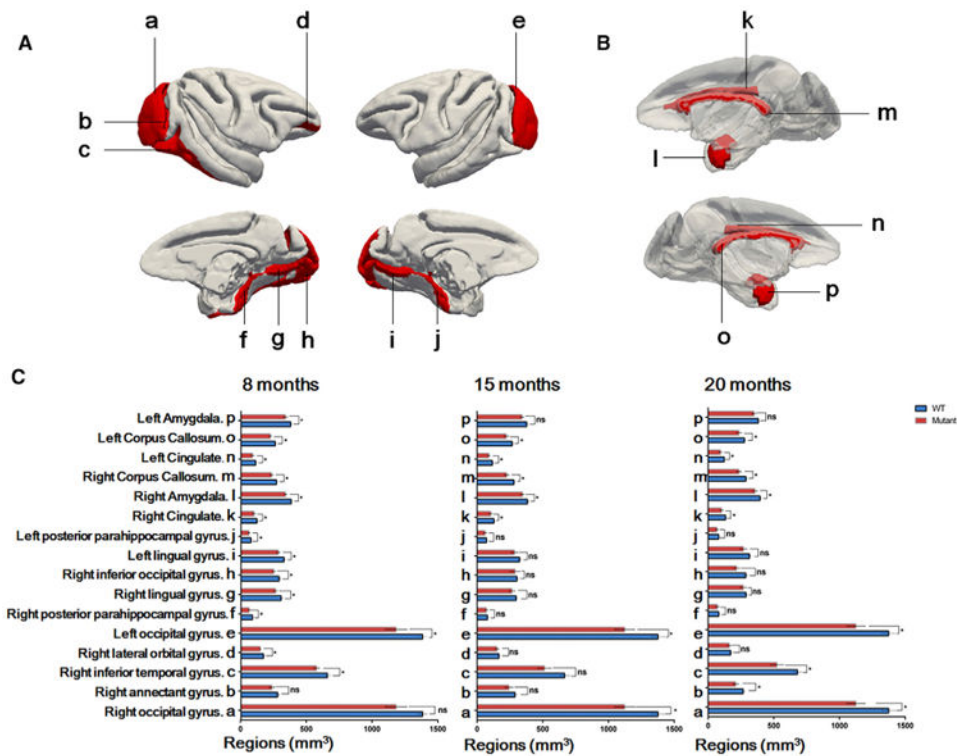
For off-target results, see also Table S3.

Figure 2. Dynamic Changes of Cortical and Sub-cortical Volume Monitored by MRI Scanning

(A) Regional measurements on cortical volume in mutant monkeys showed significantly smaller values in several regions (A), including in bilateral parahippocampal gyrus at 8 months, left lingual gyrus at 8 months, left occipital gyrus at 8, 15, and 20 months, right lateral orbital gyrus at 8 months, right inferior occipital gyrus at 8 months, right inferior temporal gyrus at 8 and 20 months, right occipital gyrus at 15 and 20 months, right annectant gyrus at 20 months, and right lingual gyrus at 20 months (a–j).

(B) Sub-cortical regional and white matter (WM) volumes measurements in mutant monkeys showed significantly smaller values in several regions, including in bilateral amygdala at 8 months, right amygdala at 15 months, bilateral cingulate WM region at 8, 15, and 20 months, and bilateral corpus callosum at 8, 15, and 20 months (k–p).

(C) Quantitative analysis for measurements of (A) and (B). Bars and error bars represent mean ± SEM of replicate measurements. $^{ns}p > 0.05$, $*p < 0.05$ (rank-sum test). For more information and further analysis, see also Figures S1 and S2. General growth and development of mutants and WT monkeys were also monitored; for the result, see also Figure S3.
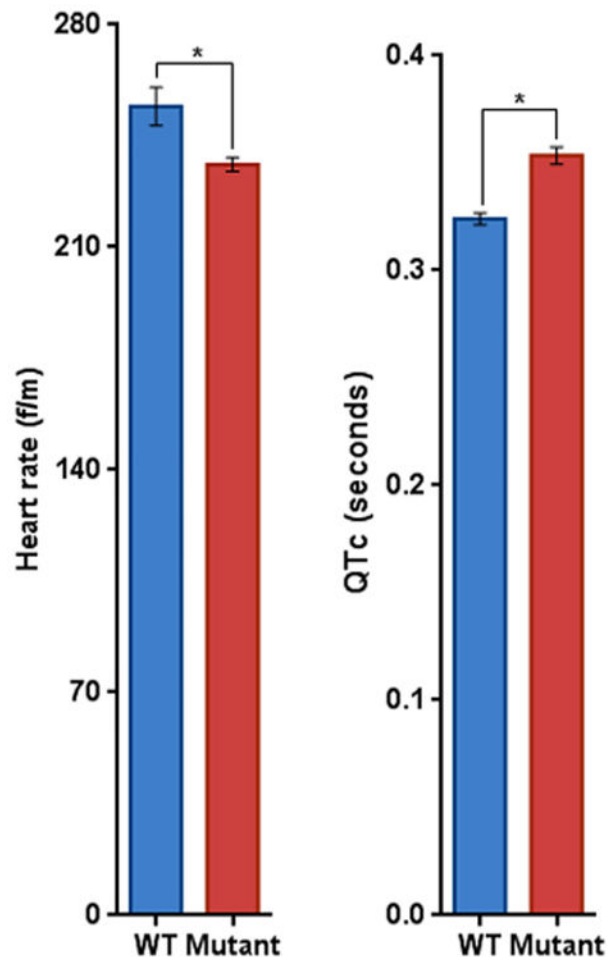
Figure 3. The EKG of *MECP2* Mutant and WT Monkeys

The heart rate (HR) and QTc of five mutants and five WT monkeys. The mean value of HR in mutants was lower than that in WT monkeys, while QTc measurements in mutants were significantly prolonged compared with WT monkeys. The normality of data for heart rate and electrocardiogram was analyzed by Kolmogorov-Smirnov test ($p > 0.05$), and one-way ANOVA was used to compare mutant monkeys with WT monkeys. f/m, frequencies per min. Bars and error bars represent mean $\pm$ SEM of replicate measurements. $*p < 0.05$ (one-way ANOVA).
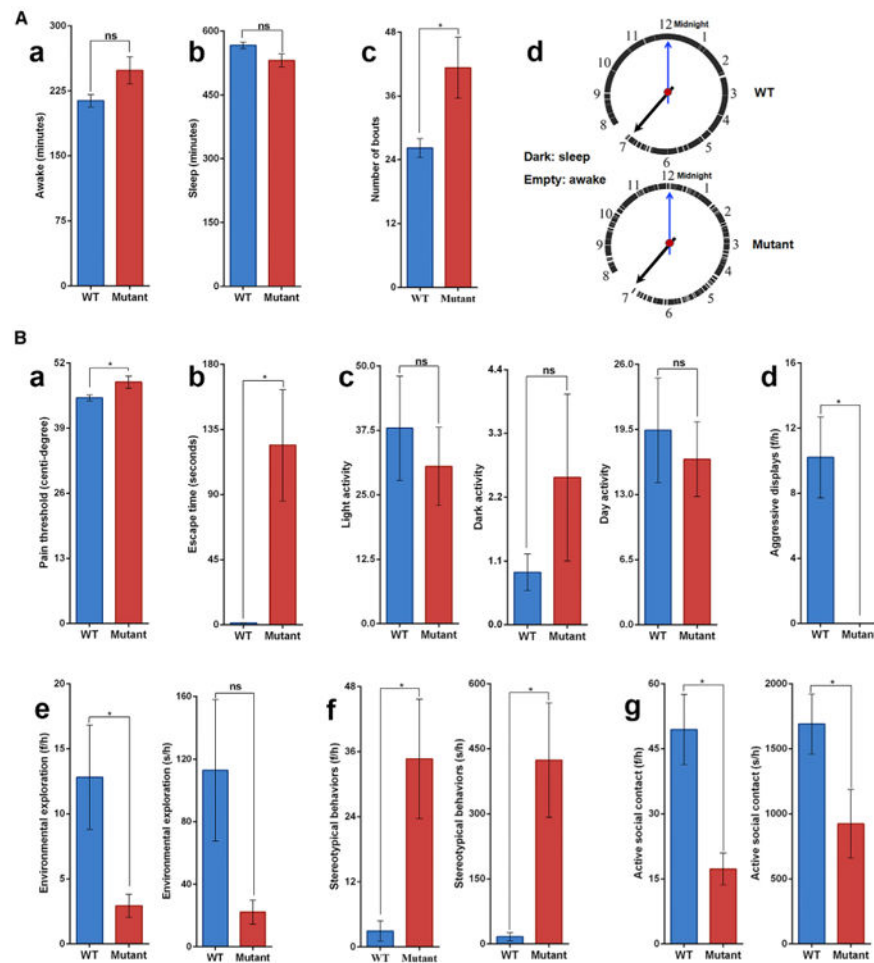
Figure 4. Behavioral Phenotypes of *MECP2* Mutant Monkeys

(A) Sleep pattern. (a and b) The mean value of awake (a) and asleep (b) durations (minutes per night) of mutant and WT monkeys. Mutant monkeys were in a longer state of awake (mutants versus WT = 248.800: 213.467 min per night, p = 0.050) and a shorter state of asleep (mutants versus WT = 531.200: 566.533 min per night, p = 0.050) than WT monkeys, but the differences have no significance (p = 0.05). (c) Sleep fragment (frequencies per night). The data suggested the mutant monkeys had trouble sleeping, as referred from the substantial number of bouts compared with WT controls (mutants versus WT = 41.333: 26.200 numbers per night, p = 0.018). (d) Video recording of an overnight alternation of sleep and wake of a random selected mutant and an age-matched WT monkey (12 hr from 7:00 p.m. to 7:00 a.m.). The patterns indicated there were more frequent naps for the mutant monkey.

(B) Responses to environments. (a) Pain perception of mutants and WT monkeys. The mutants' retarded responses to heat indicated they had a higher threshold for pain than WT controls (mutants versus WT = 48.192: 45.037°C, p = 0.030). (b) Active avoidance to noise exhibited by mutants and WT. The mutant monkeys showed delayed responses to noise, as it took longer for mutants to escape than the WT controls did (mutants versus WT = 124.067:1.267 s, p = 1.345 × 10⁻⁵). (c) Activity. Compared with WT control monkeys, mutants showed no significantly lower levels of activity during the 24 hr monitoring

(mutants versus WT = 16.522:19.412, p = 0.665). During light time (8:00–20:00), no significant difference was observed between mutants and WT controls in levels of activity (mutants versus WT = 30.504: 37.920, p = 0.574), and there was also no significant difference in dark time (20:00–8:00) activities (mutants versus WT = 2.542: 0.906,p = 0.299). (d) Aggressive behaviors. Mutant monkeys exhibited no aggressive behaviors, which was significantly different from WT controls (mutants versus WT = 0:10.200 f/h, p = 7.772 $\times 10^{-6}$). (e) Environmental exploration. Mutant monkeys exhibited less frequencies of environmental exploration than WT controls (mutants versus WT = 2.933: 12.800 f/h, p = 0.035). However, no significant difference was found in duration of environmental exploration (mutants versus WT = 22.200: 112.867 s/h, p = 0.053). (f) Stereotypical behaviors. Mutant monkeys exhibited more stereotypical behaviors than WT controls not only in frequencies (mutants versus WT = 34.667: 2.933 f/h, p = 0.021) but also in duration (mutants versus WT = 423.600: 16.667 s/h, p = 0.009). (g) Social contact. Mutant monkeys exhibited less social contact than WT controls in both frequencies (mutants versus WT = 17.267: 49.400 f/h, p = 0.001) and duration (mutants versus WT = 922.867: 1688.800 s/h, p = 0.037). All the behavioral tests above were conducted in five mutants and five age-matched WT monkeys. The "f/h" means frequencies per hour, and the "s/h" means seconds per hour.

Bars and error bars represent mean ± SEM of replicate measurements. [ns]p > 0.05, *p < 0.05 (sleep pattern, pain threshold, and active social contact, one-way ANOVA; active avoidance behavior, environmental exploration, stereotypical behaviors and aggressive displays, Wilcoxon's signed-rank tests). See also Movies S1, S2, S3, and S4.
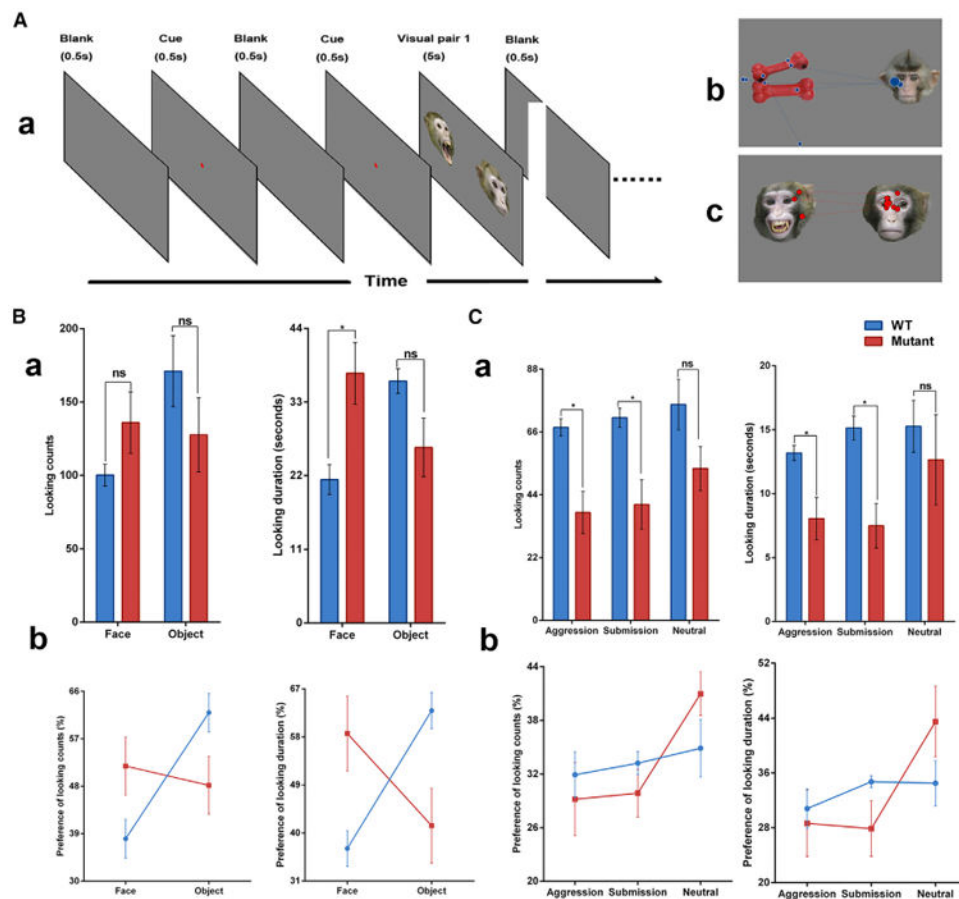
Figure 5. Eye-Tracking Patterns in *MECP2* Mutants and WT Monkeys

(A) View patterns of mutants (n = 5) and WT control monkeys (n = 5) in paired face-object task and paired emotional faces task. (a) Flow chart of eye-tracking task. The apostrophe indicates more test cycles. (b) An example of looking at one paired object-face stimuli. (c) An example of looking at one paired emotional face stimuli. The looking circle with the number "1" at the center represents the first look at this image. Subsequent looking numbered two traces the location and order of the next looks. Looking duration was in proportion to the diameter of the looking circles.

(B) Eye-tracking pattern for face-object stimuli. (a) Lines show the differences between the two groups in preference of monkey faces or objects. The mutant monkeys preferred looking at monkey faces as compared to WT controls, including looking counts (F = 8.747, p = 0.009, η_p^2 = 0.353) and looking duration (F = 15.443, p = 0.001, η_p^2 = 0.491). (b) Histograms show that differences between the two groups in looking counts and looking duration at monkey faces versus objects. No significant differences were found between two groups in looking counts, but the mutants spent more time looking at monkey faces than WT controls (F = 9.695, p = 0.014).

(C) Eye-tracking pattern for emotional faces, including aggression, submission, and neutral. (a) Lines show the differences between the two groups in preference of emotional charged faces. The mutant monkeys preferred looking at neutral faces compared with aggressive or submissive faces, but no significant differences were found between the two groups in both

looking counts (F= 1.730,p= 0.199, $\eta_p^2 = 0.126$) and looking duration (F=2.307,p=0.121, $\eta_p^2 = 0.161$). (b) Histograms show that differences between two groups in looking counts and looking duration at monkey emotional faces. The mutant monkeys looked fewer times at aggressive (F = 13.919, p = 0.006) and submissive faces (F = 10.714, p = 0.011), and shorter duration at aggressive (F = 8.473, p = 0.020) and submissive faces (F = 14.965,p = 0.005). When presented with neutral faces, no significant difference was observed between the two groups, including looking counts (F = 3.652,p = 0.092) and looking duration (F = 0.408, p = 0.541). The measurements of looking counts and looking duration were obtained from eye-tracking paradigm. Bars and error bars represent mean ± SEM of replicate measurements. [ns]p > 0.05, *p < 0.05 (two-way ANOVA for interaction test and one-way ANOVA for pairwise test). See also Movie S5.
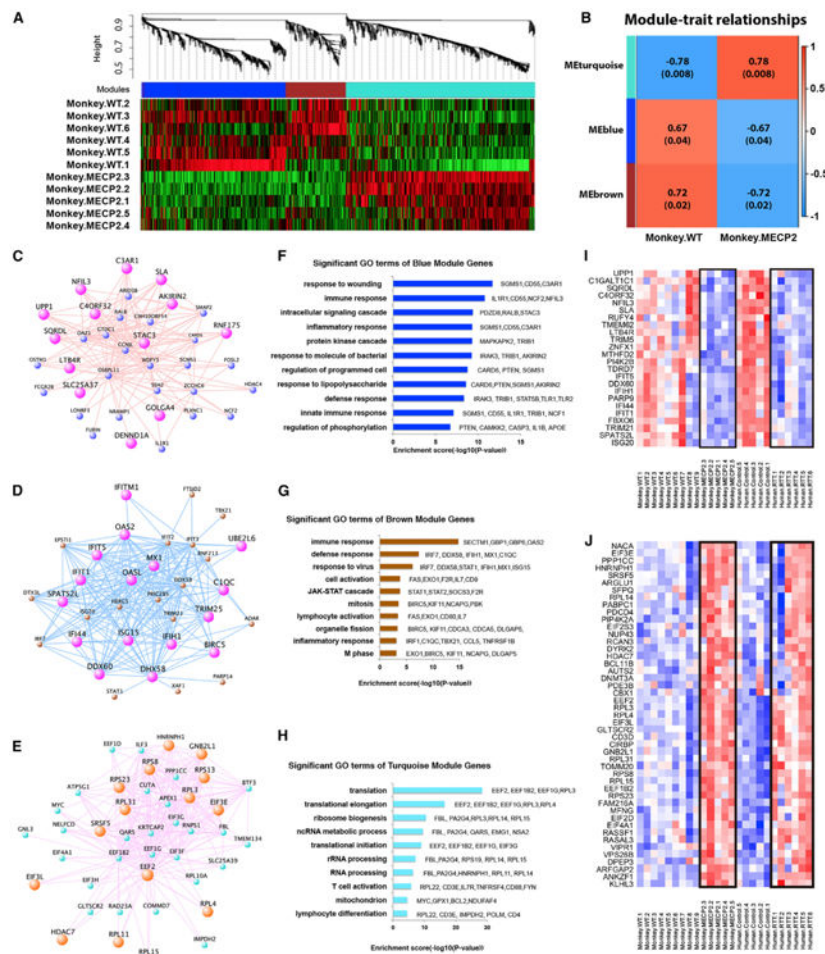
Figure 6. Gene-Network Modules Associated with *MECP2* Mutations in Monkeys and Human via WGCNA

(A) WGCNA dendrogram shows expression of different gene modules in 11 blood samples from five mutant and six WT monkeys.

(B) Correlation matrix between each module in mutant versus WT traits.

(C and D) Hub-gene network in blue (C) and brown (D) modules, respectively. Sizes of the dots correlate with degrees of hubness. Purple highlights genes shared similar changes in RTT patients.

(E) Hub-gene network in the turquoise module. Orange highlights genes shared similar changes in RTT patients.

(F–H) GO biological process term enrichment of genes in blue (F), brown (G), and turquoise (H) modules, respectively.

(I and J) Expanded view of the shared down- (I) and up- (J) regulated genes expressions in monkey and human RTT blood samples versus controls. See also Figure S4.

Key Resources Table

REAGENT or RESOURCE	SOURCE	IDENTIFIER
Antibodies		
MeCP2 (D4F3) XP(R) Rabbit mAb	Cell Signaling Technology	Cat# 3456S
TRUE-Ref Anti-GAPDH mAb	Kangcheng	Cat# KC-5G4
Goat Anti-Rabbit IgG Antibody, (H+L) HRP conjugate)	Millipore	Cat# AP307P
Goat anti-Mouse IgG, (H+L) HRP conjugate	Millipore	Cat# AP308P
Pierce[REMOVED EQ FIELD]ECL Western Blotting Substrate	Thermo Scientific	Cat#32109
Chemicals, Peptides, and Recombinant Proteins		
Paraformaldehyde	Sigma-Aldrich	Cat# 16005
Recombinant Human FSH, Gonal F	Merck Serono	Cat# Gonal-f
Recombinant Human Chorionic Gonadotropin alfa for Injection	Merck Serono	Cat# Ovidrel
Fetal bovine serum	GIBCO	Cat# 10099-141
Hamster embryo culture medium-9	Millipore	Cat# H002B
Kits and vectors		
T7 Endonuclease	NEB	Cat# M0302L
GLOBINclear kit	Life Technologies	Cat# AM1980
TruSeq RNA Library Prep Kit	Illumina	Cat# v2
T-Vector pMD20	Takara	Cat# 3270
Deposited Data		
Human subject details, see Table S4	This study	N/A
RNA-seq raw data of monkeys	NCBI Sequencing Read Archive	PRJNA383877 (https://www.ncbi.nlm.nih.gov/bioproject/383877)
RNA-seq raw data of children	NCBI Sequencing Read Archive	PRJNA383878 (https://www.ncbi.nlm.nih.gov/bioproject/383878)
Animals		
Cynomolgus monkeys	Yunnan Key Laboratory of Primate Biomedical Research	N/A
Narcotic Analgesics		
Ketamine hydrochloride	Gutian pharmaceutical, Fujian, China	Cat# 1505242
Xylazine	Huamu Animal health products, Jilin, China	Cat# 151207

REAGENT or RESOURCE	SOURCE	IDENTIFIER
Recombinant DNA		
pCS2-peas-T(MECP2-TALEN1, MECP2-TALEN2,MECP2-TALEN3)	Liu et al., 2014	N/A
Database, Software and Algorithms		
PrimFace database	N/A	https://visiome.neuroinf.jp/primface
TALENoffer	Grau et al., 2013	http://www.jstacs.de/index.php/TALENoffer
Actical(v3.1.0)	Respironics, Pennsylvania, U.S.A.	https://bmedical.com.au/product-category/activity-heat-research/actical/
Tobii Studio software	Tobii Technology AB, Danderyd, Sweden	http://acuity-ets.com/products_tobii_studio.htm
TopHat (v.2.0.12)	Trapnell et al., 2009	http://tophat.cbcb.umd.edu.
VisANT 1.0.	N/A	http://visant.bu.edu/home2.htm
False discovery rate	Benjamini and Hochberg, 1995	http://www.jstor.org/stable/2346101
Weighted Gene Coexpression Network Analyses	Zhang and Horvath, 2005	https://www.degruyter.com/view/j/sagmb.2005.4.issue-1/sagmb.2005.4.1.1128/sagmb.2005.4.1.1128
Other		
SYMTOP biophysical recording system	Symtop Instrument, China	UEA-41FZ
Laparoscopic follicular aspiration	STORZ	Hopkins II 10mm
Actical Physical Activity Monitors	Respironics, Pennsylvania, USA	N/A
Tobii Pro TX300 Eye Tracker	Tobii Technology AB, Danderyd, Sweden	TX300